HERMETIC PACKAGES AND FEEDTHROUGHS FOR NEURAL PROSTHESES

Quarterly Progress Report # 4

(Contract NIH-NINDS-N01-NS-8-2387)

(Contractor: The Regents of the University of Michigan)

For the Period:

January - March 1999

Submitted to the

Neural Prosthesis Program
National Institute of Neurological Disorders and Stroke
National Institutes of Health

By the

Center For Integrated Microsystems
Department of Electrical Engineering and Computer Science
University of Michigan
Ann Arbor, Michigan 48109-2122

Program Personnel:

UNIVERSITY OF MICHIGAN

Faculty:
Professor Khalil Najafi: Principal Investigator
Professor David J. Anderson: Biological Experiments

Staff:
Mr. James Wiler: Animal Implants and Surgery

Graduate Student Research Assistants:
Mr. Mehmet Dokmeci: Packaging and Accelerated Testing
Mr. Sebastien Hauvespre: Package Fabrication and Telemetry Testing
Mrs. Li Chen: Transmitter Design and Testing

April 1999

SUMMARY

During the past quarter we continued testing the silicon-glass packages at room temperature in saline, continued characterization of the relative humidity sensor for long term drift, assembled and tested a wireless humidity monitoring system and verified its functionality, and redesigned and implemented the external transmitter to operate at 4MHz.

In the previous quarter, we mentioned that all the ongoing packages in the de-ionized water tests have failed and a lifetime of 58 years at the body temperature is estimated from these tests. Prior to this quarter, we also had 4 packages soaking at room temperature in saline as a control group to complement the accelerated tests. In this set of tests, the longest lasting package has been soaking for 1595 days, and an average soak duration for this set so far is 1301 days. All of these 4 packages are still dry and being tested. In all of our accelerated tests, we have observed the dissolution of silicon and polysilicon at the elevated temperatures. This past quarter in order to further understand and resolve this issue, we have designed and simulated a set of conditions using a different dopant than Phosphorus (namely Boron) and different dopant densities. Dissolution studies will be conducted during the coming quarter so that we can continue our accelerated tests without any early failures. We have also finished the fabrication of 2 substrate wafers and will utilize these in Glass-Silicon package fabrication to be used for mechanical testing as well as for in-vivo tests.

We have continued characterization of the relative humidity sensor. We have found out that the sensor drifts about 2% RH in a 10-day test at 50% RH at 37°C. This is a promising result since the actual humidity sensors would be sealed at high temperature and low humidity environment of anodic sealing, we expect the drift to be much less and using this sensor one can detect humidity with very high precision.

A wireless system that consists of a hybrid coil and a polyimide relative humidity sensor has been designed, simulated and assembled together and tested. We have optimized the system parameters to maximize the magnitude of the response from the system. We then sealed the humidity sensor-hybrid coil system in our glass-silicon package using anodic bonding. Our preliminary test results demonstrate that the system works well and can be used to monitor the environment inside micropackages for a distance of up to 2cm. This system also allows automating our accelerated long term testing procedure.

The external transmitter that sends power and data to the microstimulator has been redesigned to operate at 4MHz. Further tests are underway to fully characterize the transmitter and increase its efficiency at this frequency. After accomplishing this, we hope to make several hand held transmitters and assemble and deliver low profile fully integrated systems to interested users.

I. INTRODUCTION

This project aims at the development of hermetic, biocompatible micropackages and feedthroughs for use in a variety of implantable neural prostheses for sensory and motor handicapped individuals. In addition, it will also develop a telemetry system for monitoring package humidity in unrestrained animals, and of telemetry electronics and packaging for stimulation of peripheral nerves. The primary objectives of the proposed research are: 1) the development and characterization of hermetic packages for miniature, silicon-based, implantable neural prostheses designed to interface with the nervous system for many decades; 2) the development of techniques for providing multiple sealed feedthroughs for the hermetic package; 3) the development of custom-designed packages and systems used in several different chronic stimulation or recording applications in the central or peripheral nervous systems in collaboration and cooperation with groups actively involved in developing such systems; and 4) establishing the functionality and biocompatibility of these custom-designed packages in *in-vivo* applications. Although the proposed research is focused on the development of the package and feedthroughs, it also aims at the development of inductively powered systems that can be used in many implantable recording and stimulation devices in general, and of multichannel microstimulators for functional neuromuscular stimulation, and multichannel recording microprobes for CNS applications in particular.

Our group here at the Center for Integrated Sensors and Circuits at the University of Michigan has been involved in the development of silicon-based multichannel recording and stimulating microprobes for use in the central and peripheral nervous systems. More specifically, during the past three contract periods dealing with the development of a single-channel inductively powered microstimulator, our research and development program has made considerable progress in a number of areas related to the above goals. A hermetic packaging technique based on electrostatic bonding of a custom-made glass capsule and a supporting silicon substrate has been developed and has been shown to be hermetic for a period of at least a few decades in salt water environments. This technique allows the transfer of multiple interconnect leads between electronic circuitry and hybrid components located in the sealed interior of the capsule and electrodes located outside of the capsule. The glass capsule can be fabricated using a variety of materials and can be made to have arbitrary dimensions as small as 1.8mm in diameter. A multiple sealed feedthrough technology has been developed that allows the transfer of electrical signals through polysilicon conductor lines located on a silicon support substrate. Many feedthroughs can be fabricated in a small area. The packaging and feedthrough techniques utilize biocompatible materials and can be integrated with a variety of micromachined silicon structures.

The general requirements of the hermetic packages and feedthroughs to be developed under this project are summarized in Table 1. Under this project we will concentrate our efforts to satisfy these requirements and to achieve the goals outlined above. There are a variety of neural prostheses used in different applications, each having different requirements for the package, the feedthroughs, and the particular system application. The overall goal of the program is to develop a miniature hermetic package that can seal a variety of electronic components such as capacitors and coils, and integrated circuits and sensors (in particular electrodes) used in neural prostheses. Although the applications are different, it is possible to identify a number of common requirements in all of these applications in addition to those requirements listed in Table 1. The packaging and feedthrough technology should be capable of:

1- protecting non-planar electronic components such as capacitors and coils, which typically have large dimensions of about a few millimeters, without damaging them;
2- protecting circuit chips that are either integrated monolithically or attached in a hybrid fashion with the substrate that supports the sensors used in the implant;
2 interfacing with structures that contain either thin-film silicon microelectrodes or conventional microelectrodes that are attached to the structure;

Table 1: General Requirements for Miniature Hermetic Packages and Feedthroughs for Neural Prostheses Applications.

Package Lifetime:

≥ 40 Years in Biological Environments @ 37°C

Packaging Temperature:

≤360°C

Package Volume:

10-100 cubic millimeters

Package Material:

Biocompatible
Transparent to Light
Transparent to RF Signals

Package Technology:

Batch Manufactureable

Package Testability:

Capable of Remote Monitoring
In-Situ Sensors (Humidity & Others)

Feedthroughs:

At Least 12 with ≤125μm Pitch
Compatible with Integrated or Hybrid Microelectrodes
Sealed Against Leakage

Testing Protocols:

In-Vitro Under Accelerated Conditions
In-Vivo in Chronic Recording/Stimulation Applications

We have identified two general categories of packages that need to be developed for implantable neural prostheses. The first deals with those systems that contain large components like capacitors, coils, and perhaps hybrid integrated circuit chips. The second deals with those systems that contain only integrated circuit chips that are either integrated in the substrate or are attached in a hybrid fashion to the system.

Figure 1 shows our general proposed approach for the package required in the first category. This figure shows top and cross-sectional views of our proposed approach here. The package is a glass capsule that is electrostatically sealed to a support silicon substrate. Inside the glass capsule are housed all of the necessary components for the system. The electronic circuitry needed for any analog or digital circuit functions is either fabricated on a separate circuit chip that is hybrid mounted on the silicon substrate and electrically connected to the silicon substrate, or integrated monolithically in the support silicon substrate itself. The attachment of the hybrid IC chip to the silicon substrate can be performed using a number of different technologies such as simple wire bonding between pads located on each substrate, or using more sophisticated techniques such as flip-chip solder reflow or tab bonding. The larger capacitor or microcoil components are mounted on either the substrate or the IC chip using appropriate epoxies or solders. This completes the assembly of the electronic components of the system and it should be possible to test the system electronically at this point before the package is completed. After testing, the system is packaged by placing the glass capsule over the entire system and bonding it to the silicon substrate using an electrostatic sealing process. The cavity inside the glass package is now hermetically sealed against the outside environment. Feedthroughs to the outside world are provided using the grid-feedthrough technique discussed in previous reports. These feedthroughs transfer the electrical signals between the electronics inside the package and various elements outside of the package. If the package has to interface with conventional microelectrodes, these microelectrodes can be attached to bonding pads located outside of the package; the bond junctions will have to be protected from the external environment using various polymeric encapsulants. If the package has to interface with on-chip electrodes, it can do so by integrating the electrode on the silicon support substrate. Interconnection is simply achieved using on-chip polysilicon conductors that make the feedthroughs themselves. If the package has to interface with remotely located recording or stimulating electrodes that are attached to the package using a silicon ribbon cable, it can do so by integrating the cable and the electrodes again with the silicon support substrate that houses the package and the electronic components within it.

Figure 2 shows our proposed approach to package development for the second category of applications. In these applications, there are no large components such as capacitors and coils. The only component that needs to be hermetically protected is the electronic circuitry. This circuitry is either monolithically fabricated in the silicon substrate that supports the electrodes (similar to the active multichannel probes being developed by the Michigan group), or is hybrid attached to the silicon substrate that supports the electrodes (like the passive probes being developed by the Michigan group). In both of these cases the package is again another glass capsule that is electrostatically sealed to the silicon substrate. Notice that in this case, the glass package need not be a high profile capsule, but rather it need only have a cavity that is deep enough to allow for the silicon chip to reside within it. Note that although the silicon IC chip is originally 500μm thick, it can be thinned down to about 100μm, or can be recessed in a cavity created in the silicon substrate itself. In either case, the recess in the glass is less than 100μm deep (as opposed to several millimeters for the glass capsule). Such a glass package can be easily fabricated in a batch process from a larger glass wafer.

The above two approaches address the needs for most implantable neural prostheses. Note that both of these techniques utilize a silicon substrate as the supporting base, and are not directly applicable to structures that use other materials such as ceramics or metals. Although this may seem a limitation at first, we believe that the use of silicon is, in fact, an advantage because it is biocompatible and many emerging systems use silicon as a support substrate.

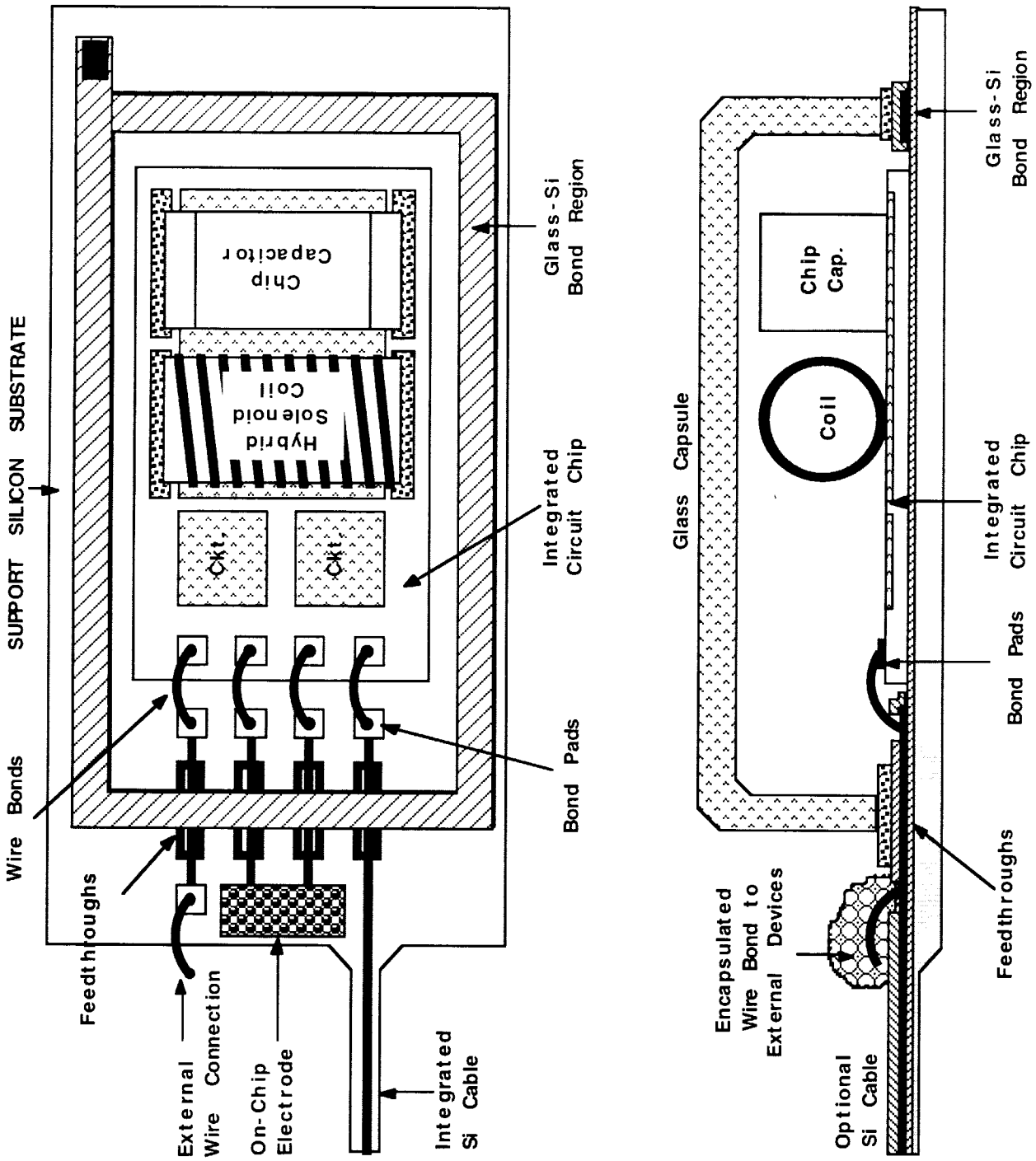

Figure 1: A generic approach for packaging implantable neural prostheses that contain a variety of components such as chip capacitors, microcoils, and integrated circuit chips. This packaging approach allows for connecting to a variety of electrodes.

We will further improve the silicon glass package and its built-in feedthroughs, and will study and explore alternative technologies for hermetic packaging of implantable systems. In particular, we have proposed using a silicon capsule that can be electrostatically bonded to a silicon substrate thus allowing the capsule to be machined down to dimensions below a 100μm. We will also develop an implantable telemetry system for monitoring package humidity in unrestrained animals for a period of at least one year. Two separate systems have been proposed, one based on a simple oscillator, and the other based on a switched-capacitor readout interface circuit and an on-chip low-power AD converter, both using a polyimide-based humidity sensor. This second system will telemeter the humidity information to an outside receiver using a 300MHz on-chip transmitter.

Finally, we have forged potential collaborations with two groups working in the development of recording/stimulating systems for neural prostheses. The first group is that led by Professor Ken Wise at the University of Michigan, which has been involved in the development of miniature, silicon-based multichannel recording and stimulation system for the CNS for many years. Through this collaboration we intend to develop hermetic packages and feedthroughs for a 3-D recording/stimulation system that is under development at Michigan. We will also develop the telemetry front end necessary to deliver power and data to this system. The second group is at Case Western Reserve University, led by Prof. D. Durand, and has been involved in recording and stimulation from peripheral nerves using cuff electrodes. Through this collaboration we intend to develop a fully-integrated, low-profile, multichannel, hermetic, wireless peripheral nerve stimulator that can be used with their nerve cuff electrode. This system can be directly used with other nerve cuffs that a number of other groups around the country have developed. Both of these collaborations should provide us with significant data on the reliability and biocompatibility of the package.

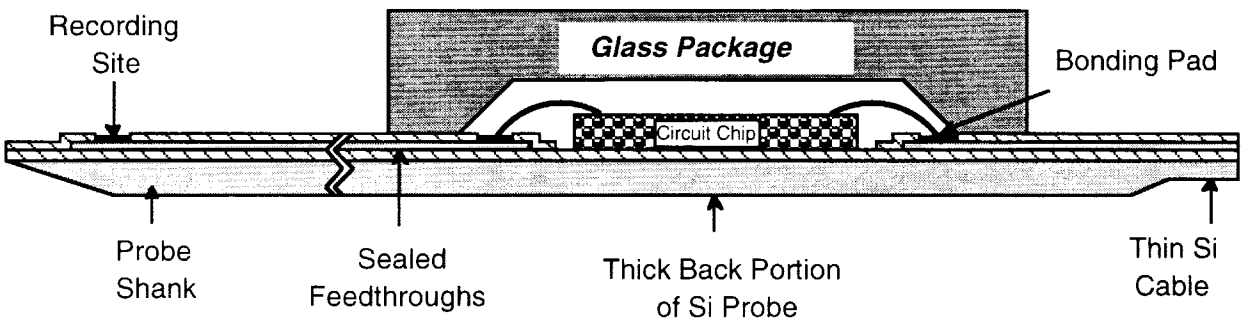

Figure 2: Proposed packaging approach for implantable neural prostheses that contain electronic circuitry, either monolithically fabricated in the probe substrate or hybrid attached to the silicon substrate containing microelectrodes.

II. ACTIVITIES DURING THE PAST QUARTER

2.1 Hermetic Packaging

Over the past few years we have developed a biocompatible hermetic package with high density multiple feedthroughs. This technology utilizes electrostatic bonding of a custom-made glass capsule to a silicon substrate to form a hermetically sealed cavity, as shown in Figure 3. Feedthrough lines are obtained by forming closely spaced polysilicon lines and planarizing them with LTO and PSG. The PSG is reflowed in steam at 1100°C for 2 hours to form a planarized surface. A passivation layer of oxide/nitride/oxide is then deposited on top to prevent direct exposure of PSG to moisture. A layer of fine-grain polysilicon (surface roughness 50Å rms) is deposited and doped to act as the bonding surface. Finally, a glass capsule is bonded to this top polysilicon layer by applying a voltage of 2000V between the two for 10 minutes at 320 to 340°C, a temperature compatible with most hybrid components. The glass capsule can be either custom molded from Corning code #7740 glass, or can be batch fabricated using ultrasonic micromachining of #7740 glass wafers.

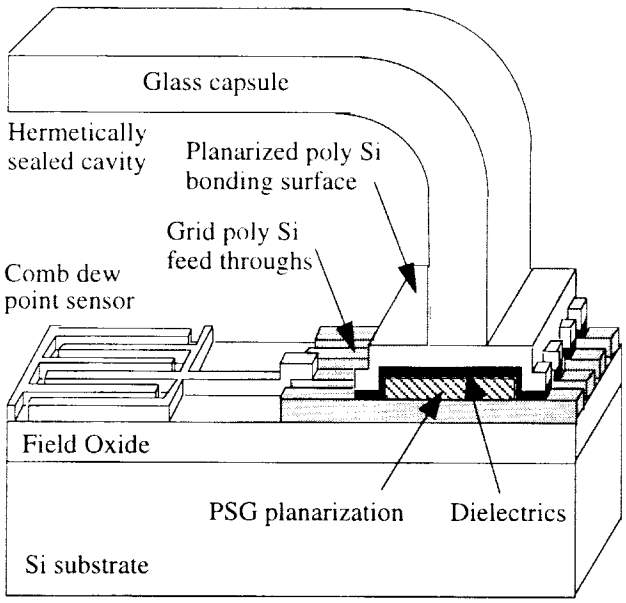

Figure 3: The structure of the hermetic package with grid feedthroughs.

During the past few years we have electrostatically bonded and soak tested over one hundred and sixty of these packages. The bonding yield is about 82% (yield is defined as the percentage of packages which last more than 24 hours in the solution they are soaked in). At the beginning of this quarter 4 devices were still being tested in saline at room temperature. These devices have been under test for more than 4 years and show no sign of leakage. We should mention that these devices have been made with silicon substrates that are thinned (~150μm) and bonded to the custom molded glass capsules. During this quarter we also looked into ways to stop dissolution of polysilicon and have now considered the use of boron-doped polysilicon as a means to prevent dissolution. We have performed computer simulations and designed various dopant densities for the polysilicon layer. Once we resolve the problem of dissolution we will start a new batch of accelerated tests. We have also continued fabrication of silicon substrates and are about to begin in-vivo tests using a wireless humidity sensor-hybrid coil system.

2.1.1 Ongoing Room Temperature Soak Tests in Saline

The packages soaked in phosphate buffered saline at room temperature have been under test for more than 4 years now. These soak tests were started to complement the accelerated soak tests at the higher temperatures. We have consistently observed in these tests that at room temperature we are below the activation energy required to cause dissolution of polysilicon and hence we have not yet observed any dissolution related failures. This result is in accordance with the acceleration model used in interpreting the high temperature tests. Indeed, it seems to confirm that the activation energy for the dissolution of the substrate or the top polysilicon is high. Accordingly, due to the exponential decrease of the acceleration factor with temperature, the dissolution of silicon or polysilicon may not be significant at the body temperature.

Out of the original 6 packages, one failed prematurely the first day and one failed because of mishandling. The 4 other devices are still under test and present no sign of leakage into the capsule after being soaked for 1595 days. Table 2 summarizes the data obtained from these soak tests.

Table 2: Data for room temperature soak tests in saline.

Number of packages in this study	6
Soaking solution	Saline
Failed within 24 hours (not included in MTTF)	1
Packages lost due to mishandling	1
Longest lasting packages in this study	1595 days
Packages still under tests with no measurable room temperature condensation inside	4
Average lifetime to date (MTTF) so far including losses due to mishandling	1300.8 days
Average lifetime to date (MTTF) so far excluding losses due to mishandling	1595 days

2.2 Preventing Dissolution of Polysilicon in Elevated Temperature Soak tests in Phosphate Buffered Saline

In all of our previous accelerated soak tests, the samples prematurely failed due to the dissolution of silicon or polysilicon in the slightly basic phosphate buffered saline solution. Even though this dissolution is insignificant at the body temperature, it has been the major failure mode in the high temperature tests. In the majority of the cases, the problem has occurred in the top polysilicon bonding layer that is directly exposed to the solution. The doping concentration in polysilicon significantly affects the surface roughness and hence this top layer is only lightly doped. The etch stop characteristics of heavily boron-doped silicon in KOH and EDP as a function of boron concentration have been studied and characterized by other investigators [1] and widely utilized in making micromachined sensors and transducers [2,3]. Traditionally, most of these studies are performed with solid state Boron diffusion, a requirement to achieve robust and hence thicker structures; however recently ion implantation has also been utilized to create etch stop layers and micromachined sensors [4]. It is very likely that one can prevent the dissolution of polysilicon in saline using a heavily-boron-doped polysilicon layer. High-temperature diffusion will increase the surface roughness, which could compromise the hermeticity. Accordingly, we are exploring

the use of ion implanted polysilicon films to prevent dissolution without sacrificing surface roughness. For this set of experiments a group of wafers have been oxidized (to a thickness of 1 micron) for isolation from the substrate and fine-grain polysilicon of thickness 1 micron is next deposited on top. The simulation results in Figure 4 shows the doping profile in the polysilicon after it is implanted with Boron at a dose of 1E16 and an Energy of 90KeV. also shown is the doping profile after the annealing step at 1075°C for 15 minutes. Another set of wafers will be implanted at a dose of 1E14 and an energy of 140KeV. Figure 5 shows the profile as implanted and after annealing at 1075°C for 15 minutes. In these tests, we will inspect the surface roughness arising from ion implantation with different doses and energies and also characterize the etch rates of polysilicon with different doping densities in saline at elevated temperatures. The results from these tests will be reported in the coming quarter.

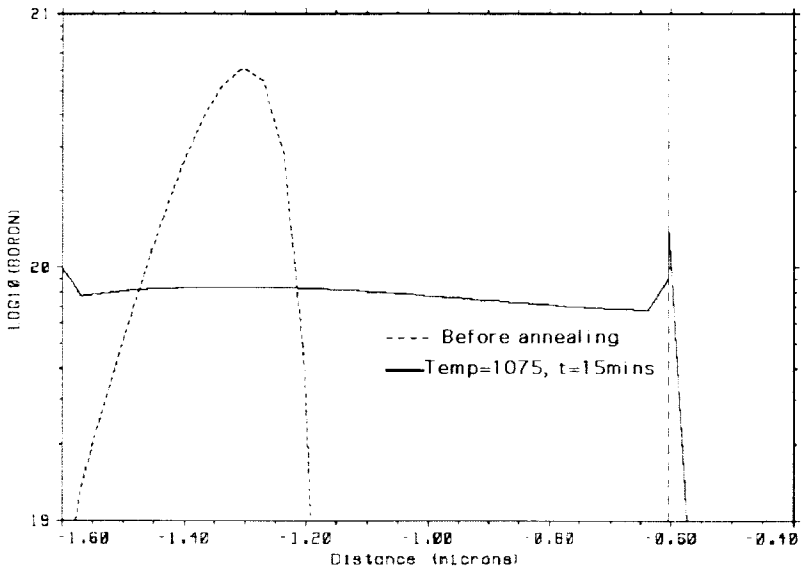

Figure 4: Profile of ion implanted Boron (Dose=1e16, Energy=90KeV) as implanted and after an anneal at 1075°C for 15 minutes.

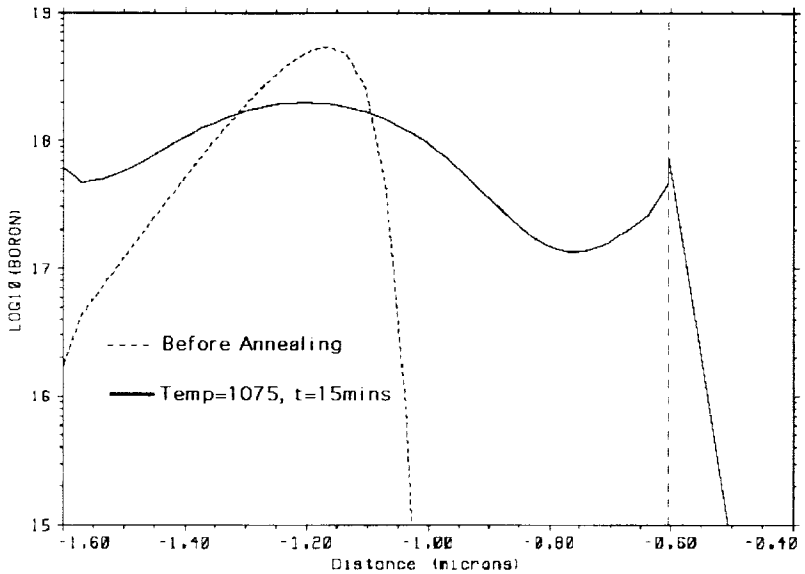

Figure 5: Profile of ion implanted Boron profile (Dose=1e14, Energy=140KeV) as implanted and after an anneal at 1075°C for 15 minutes.

2.3 Drift Studies With the Relative Humidity Sensor

In previous reports, we presented the design, fabrication and test results from the capacitive polyimide relative humidity sensor. This relative humidity sensor can be utilized as part of an active relative humidity sensing system or it can function as a part of a passive telemetric system that can record the amount of humidity inside packages implanted into animals. A photograph of the fabricated device is shown in Figure 6.

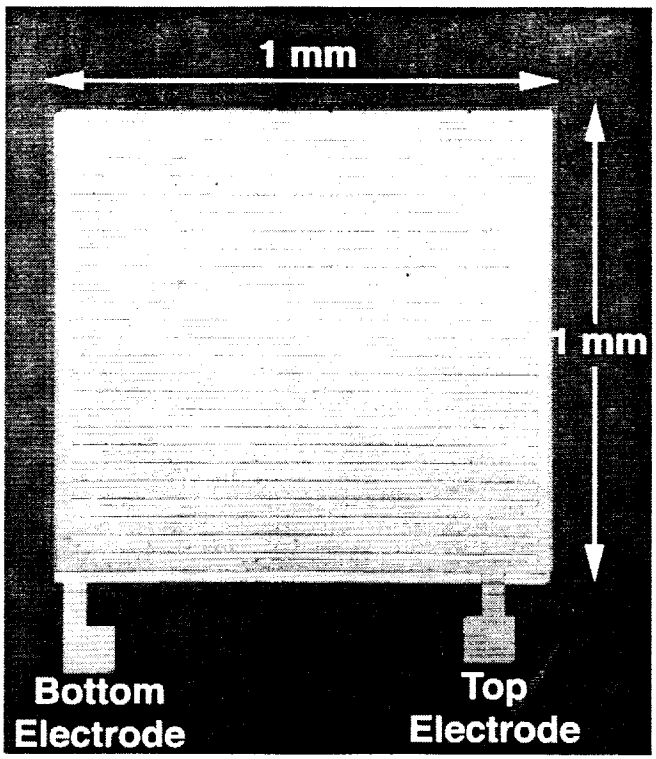

Figure 6: The photograph of the relative humidity sensor.

Once the sensor is sealed inside the glass-silicon package, it is not accessible for calibration and hence it is important that it shows little or no drift. In the previous report we presented preliminary drift studies (as long as 48 hours) at 37°C with the polyimide relative humidity sensor.

This past quarter, we have tested a 1200Å-thick polyimide sensor at 37°C for 240 hours (10 days) under 50% RH conditions, and the result from this test is shown in Figure 7. The maximum drift after 10 days was approximately 2pF which corresponded to about 2.2% RH. On the average, the drift is about 0.2pF/day which corresponds to about 6pF/month (~6.6% RH). We should also add that this device was not exposed to the anodic bonding conditions. For the actual devices which will be bonded (exposed to 340°C for 20 minutes) and hence sealed at this high temperature with less moisture present inside the package; the actual drift is expected to be much less hence the sensor could be utilized reliably for long term tests. We have developed a wireless system that can remotely monitor humidity from hermetically sealed glass-silicon packages using anodic bonding which will be detailed in the following section. In the coming quarter, using this wireless system we will conduct longer term stability tests.

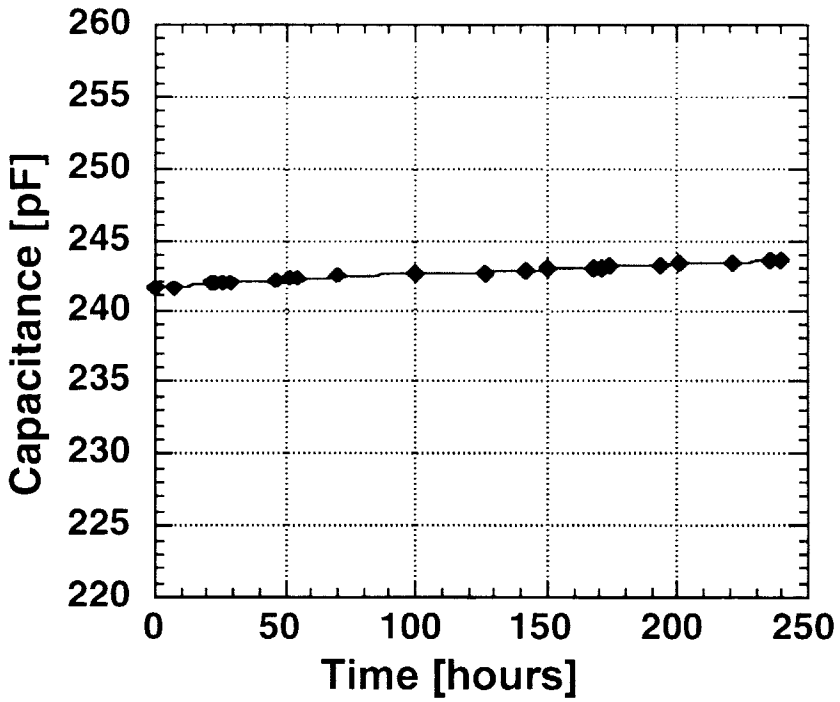

Figure 7: Stability results from a 1200Å device tested at 50% RH for 10 days at 37°C.

2.4 Wireless Monitoring of Humidity Inside the Glass-Silicon Packages

A wireless humidity monitoring system has several benefits. First, it greatly facilitates the in-vitro testing of the packages, increasing the detection threshold of moisture and reducing mishandling and temperature cycles. In addition, it allows one to automate the in-vitro testing procedure. Another benefit is that it allows monitoring of humidity in packages that are implanted in animal hosts, thus provide us with important in-vivo hermeticity data.

In the previous quarterly report, we discussed the approach that we decided to use, which can be summarized as the following: a polyimide humidity sensor which has been previously developed [5], is mounted inside the Glass-Silicon package. The capacitance of the relative humidity sensor varies from 260pF to 320pF as the humidity increases from 20 to 80%. This humidity sensor is then wire bonded to a solenoid coil. This system (inside the package) is a simple LC tank whose frequency shifts with a change in humidity. The change in the capacitance of the humidity sensor in turn changes the resonance frequency of the LC tank circuit. This frequency shift is detected using an antenna placed in the vicinity of the package, whose impedance is affected by the reflected load impedance due to the internal LC tank. At the resonance of the LC tank, the loading in the response of the outside antenna would be maximum.

In the following sub-sections, we will first provide some theoretical background and simulations, then show how this approach was implemented to fit our application and then present the test results.

In a previous quarterly progress report we presented the use of an integrated coil to implementing this wireless system. Such a system was prepared using an integrated copper coil of 10 to 17 turns, with each turn that is 20 to 40μm wide and approximately 8μm thick. However, the measured sensitivity of the system was rather poor, due to the high series resistance of the coil

and the low coupling between the external antenna, and hence we decided to replace the integrated coil with the hybrid coil. Indeed, a small hybrid coil, as described in the following section, which fits in the glass package worked well and provided good coupling to the external antenna.

2.4.1 Telemetry Modeling and Equations

System configuration

The wireless monitoring system consists of an external antenna (of inductance L_a), tightly coupled to the humidity sensing system, made of a hybrid coil (inductance L and resistance R) in parallel to a humidity sensor (whose capacitance C varies with humidity). The hybrid coil inside the package is modeled as a solenoid (a valid approximation since the actual coil has a rectangular shape) and for simplicity, we assume that the 2 coils are coaxial.

The system schematic is shown in Figure 8. We detect the reflected load impedance of the LC tank inside the package by monitoring the impedance of the external antenna. The parameters used in the equations are given in Table 3.

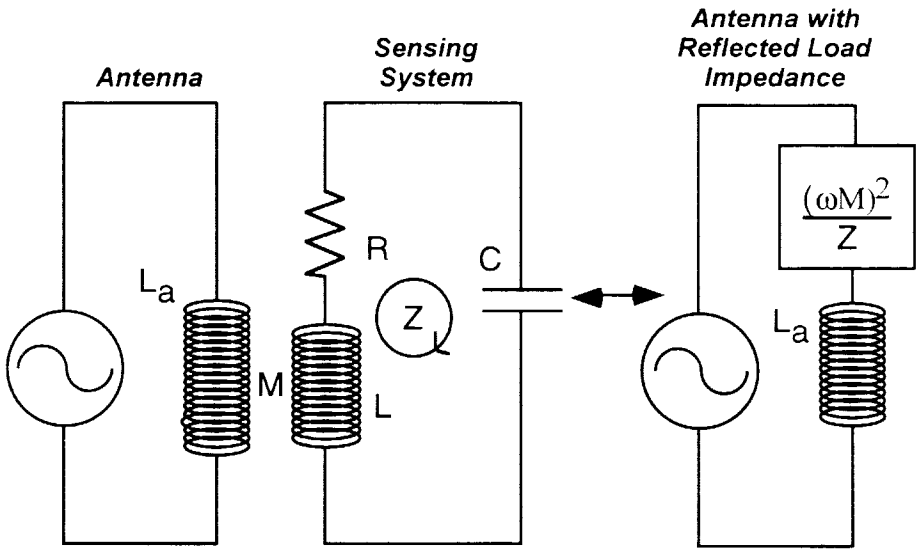

Figure 8: System configuration.

Table 3: Parameters used in the equations.

Antenna:	Humidity sensing system:
L_a self-inductance (H)	L coil self-inductance (H)
a radius (m)	d coil diameter (m)
N_a number of turns	l coil length (m)
μ_o permeability (4πe-7 Ohms/m)	S cross sectional area (m^2)
l_a Coil Length	$\mu=\mu_o\mu_r$ permeability
	μ_r relative permeability of the core
Coupling:	C capacitance of the humidity sensor
M mutual inductance	R total resistance
z axis distance	N Number of Turns

Mutual inductance calculations

We calculate the mutual inductance from the magnetic flux (B_{as}) created by the antenna in the sensor coil by a current I, divided by I:

$$M = \frac{N}{I}\int_S B_{as} \cdot ds$$

For a circular loop (radius a) carrying a current I, we have on the z-axis [7],

$$H(z) = \frac{I \cdot a^2}{2(a^{2+}z^2)^{3/2}}[A/m]$$

So the magnetic flux going through the sensor hybrid coil is given by (this value is considered to be constant because of the rather small dimensions of the hybrid coil)

$$B(z) = \mu \cdot H(z) = \frac{N_a \cdot \mu \cdot I \cdot a^2}{2(a^2 + z^2)^{3/2}} \qquad \text{(Eq.1)}$$

From which we get the mutual inductance, which is given by

$$M(z) = \frac{\mu \cdot a^2 \cdot N \cdot N_a \cdot S}{2(a^2 + z^2)^{3/2}}[Henry] \qquad \text{(Eq.2)}$$

The above formula is valid for a single or few-turn antenna, and whatever kind of hybrid coil, whose dimensions are considered smaller than the antenna.

Self-inductance calculations

For the hybrid coil, we use the empirical formula, giving the self-inductance of a solenoid,

$$L = \frac{\mu \cdot N^2 \cdot S}{l + 0.45d} \qquad \text{(Eq.3)}$$

For the antenna, we calculate a very approximate self-inductance by considering the magnetic field, calculated on the axis, as uniform on other points, that is, for a single or a few-turn coil (by having z=0 in Eq. 1),

$$B = B(z=0) = \frac{\mu \cdot N_a \cdot I}{2a}$$

So we have

$$L_a = \frac{B}{I} \cdot N_a \cdot S_a, \quad \text{where} \quad S_a = \pi \cdot a^2$$

Which finally results in:

$$L_a = \frac{\pi \cdot \mu_o \cdot N_a^2 \cdot a}{2} \qquad \text{(Eq. 4)}$$

Impedance

The impedance seen at the antenna is given by:

$$Z(\omega) = \frac{-L_a \cdot C \cdot R \cdot \omega^2 + j\left[L_a \cdot \omega + C \cdot \omega^3 \cdot M^2 - L_a \cdot \omega^3 \cdot L \cdot C\right]}{1 - L \cdot C \cdot \omega^2 + j \cdot R \cdot C \cdot \omega} \qquad \text{(Eq.5)}$$

From which we get the phase

$$\varphi(\omega) = \tan^{-1}\left(\frac{L_a \cdot \omega + C \cdot \omega^2 \cdot M^2 - L_a \cdot \omega^3 \cdot L \cdot C}{-L_a \cdot R \cdot C \cdot \omega^2}\right) - \tan^{-1}\left(\frac{R \cdot C \cdot \omega}{1 - L \cdot C \cdot \omega^2}\right) \qquad \text{(Eq.6)}$$

From Eq. 5, at resonance we have:

$$Z_{resonance} = \frac{\omega^2 \cdot M^2}{R} + j \cdot L_a \cdot \omega$$

To obtain the maximum phase dip (or highest sensitivity) we want to maximize the real part of the last expression and minimize the imaginary part. The phase deviates from 90°, as shown in Figure 9. The phase is proportional to the following parameters:

$$\varphi \propto \tan^{-1}\left(\frac{a^3 R C^{1/2}}{N}\right)$$

So, to obtain a phase as close to 0° as possible, we need to minimize R, a, C, and maximize N.

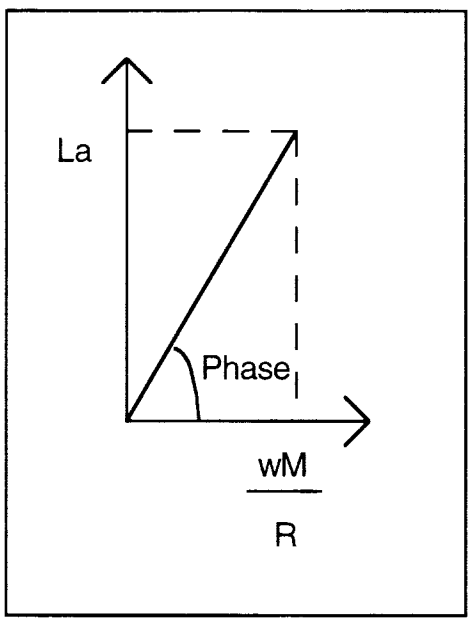

Figure 9: Phase at resonance.

2.4.2 Simulations

Using the previous equations, the relationship between the phase response of the antenna and the system parameters (N, R, C, a, z and N_a) is obtained by computer simulations (Matlab).

The nominal values used in these simulations are:

R=7 Ohms; N=20 turns; N_a=1turn; z=0; a=2 cm; C=250 pF.

In each simulation only one parameter is changed to observe its effect on the amplitude of the phase dip. Figure 10 to Figure 14 show the outcome of these results. The purpose of these simulations is to help us optimize the design of the system by identifying the parameters which will have the most important effect on the sensitivity. For instance, we see that an increase of the hybrid coil resistance from 7 to 20Ω significantly decreases the dip amplitude. This is the reason why we decided, for now, to use a hybrid coil, made of low-resistance copper wire wound around a ferrite coil instead of an integrated coil.

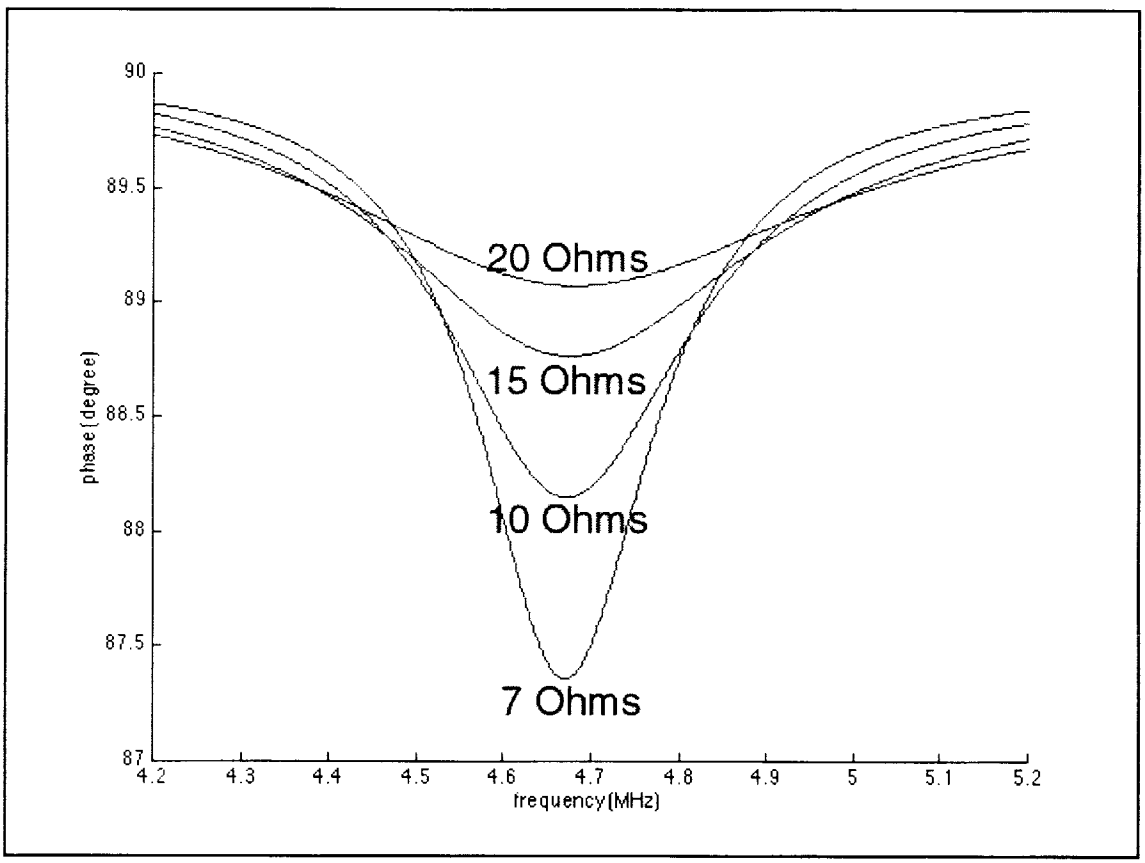

Figure 10: Simulated phase response of the antenna as R varies from 7 to 20 Ohms.

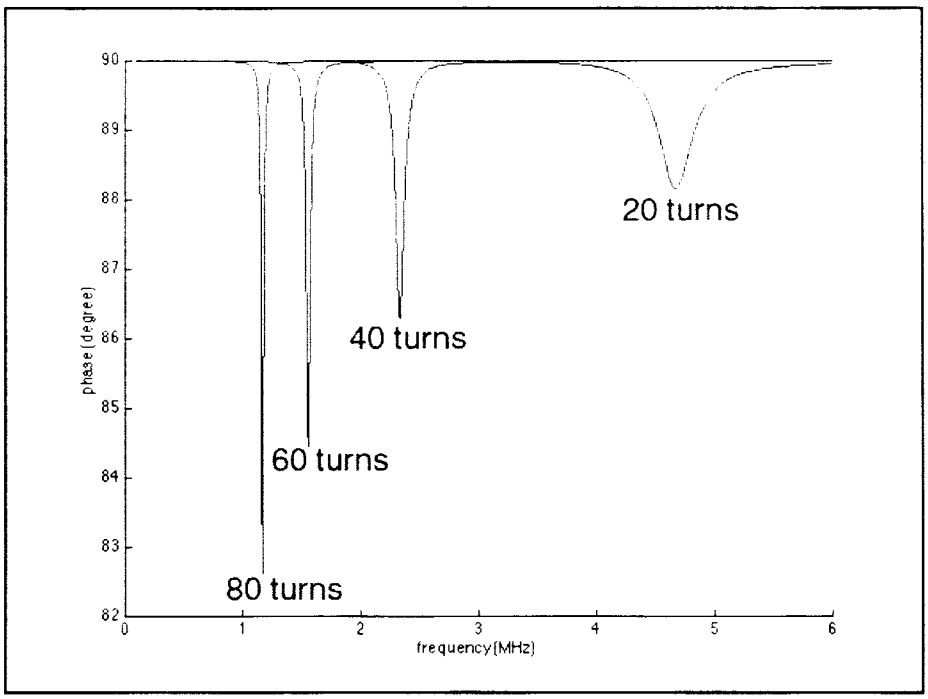

Figure 11: Simulated phase response of the antenna as N varies from 20 to 80 turns.

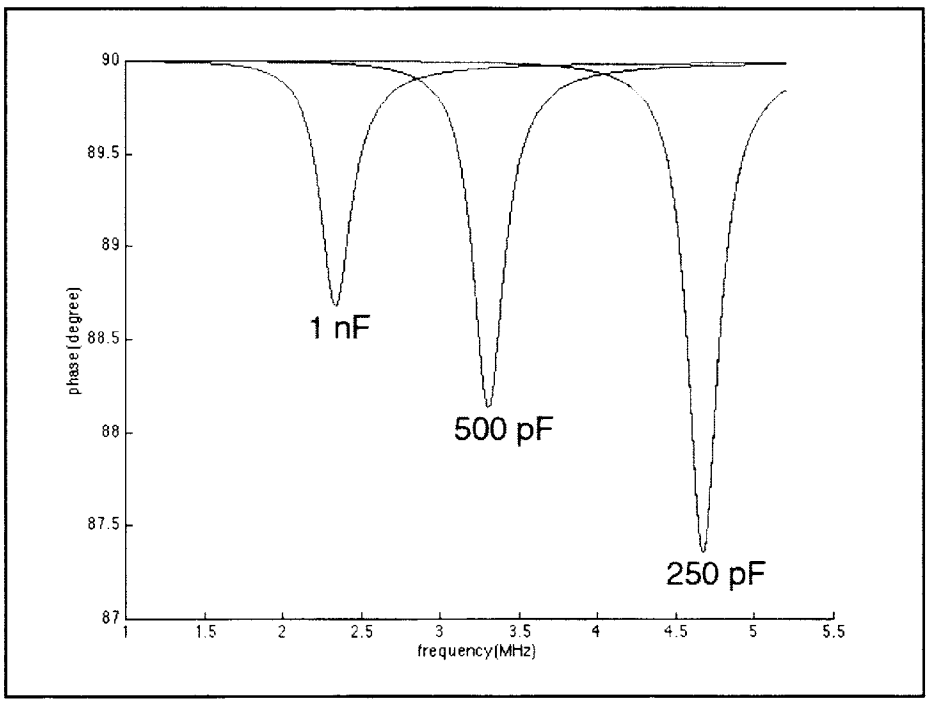

Figure 12: Simulated phase response of the antenna as C varies from 250pF to 1 nF.

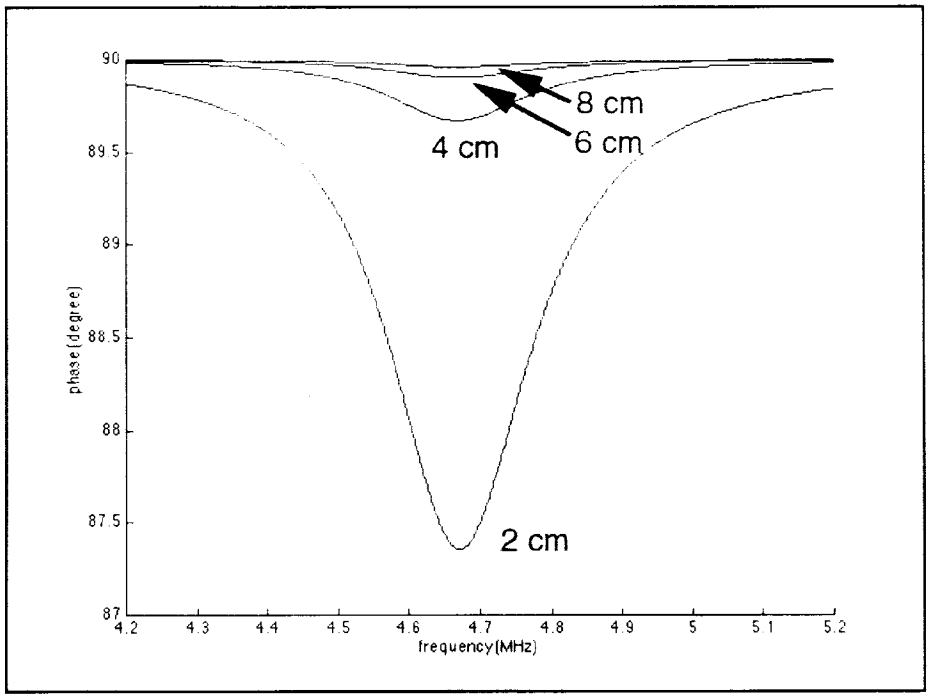

Figure 13: Simulated phase response of the antenna as a varies from 2 to 8 cm.

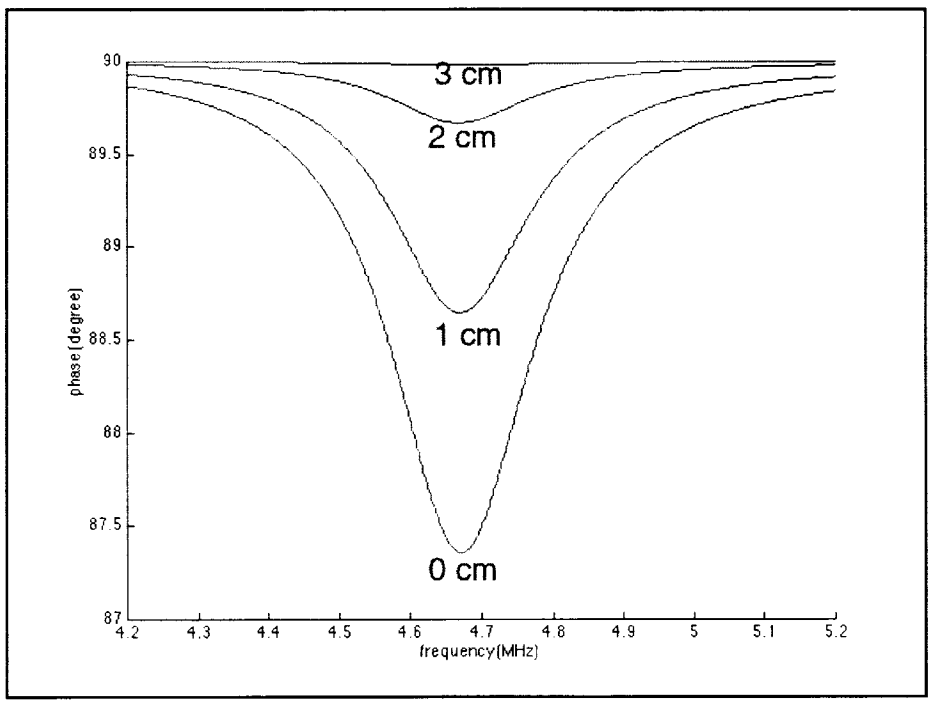

Figure 14: Simulated phase response of the antenna as z varies from 0 to 4 cm.

2.4.3 Implementation of the System and Results

As an initial attempt, a 25-turn solenoid coil wound around a 1mm-diameter, 2.5mm-length ferrite core is used for the internal coil. We later used a rectangular copper coil (with dimensions 1mmx1mmx6.5mm), making wire bonding the humidity sensor to this coil much simpler. However, there is little difference between these two systems, and we show results obtained from both of them.

Figure 15 illustrates a drawing of the system and Figure 16 shows a SEM micrograph of an assembled coil-humidity sensor placed inside the capsule (the glass is diced in half so that one can see the components inside). The ferrite core is 1mm thick. The humidity sensor can either be placed on the top (as seen on the drawing), making the thickness of the total system 1.5mm, or inserted inside a recess in the ferrite core, resulting in a total thickness of 1mm.

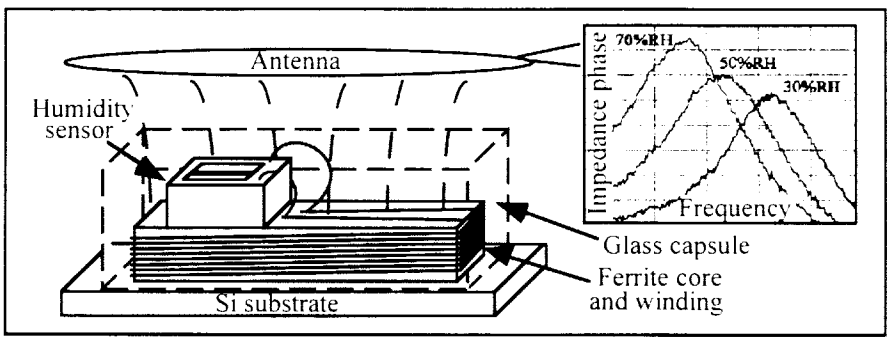

Figure 15: Humidity sensing system with the external antenna on top.

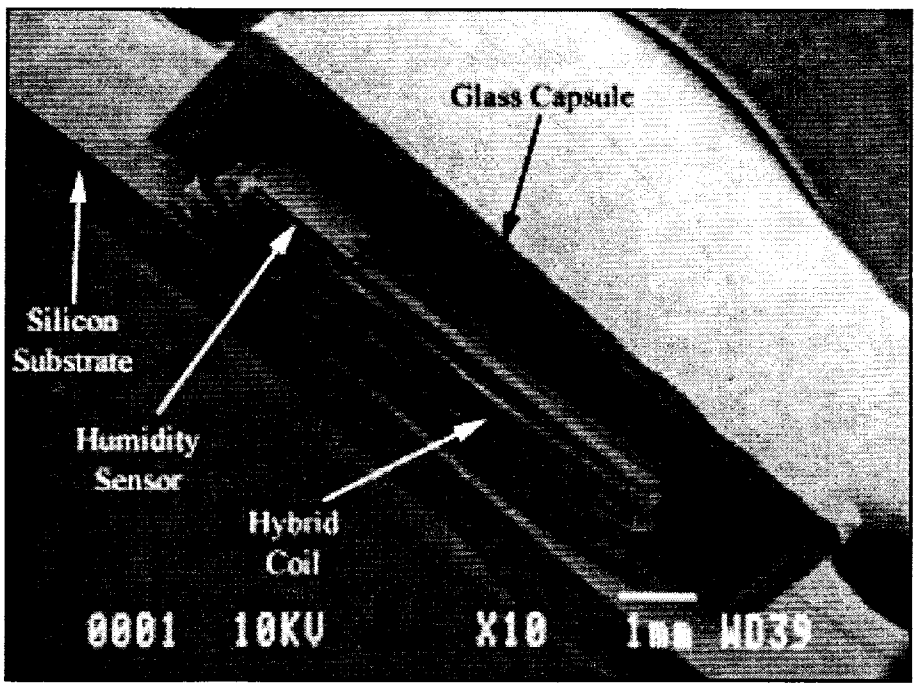

Figure 16: SEM micrograph of the humidity sensor-hybrid coil system inside a half-diced glass capsule.

The equations derived in section 2.4.1 predict a phase dip of the antenna impedance at the resonance frequency of the LC tank. Figure 17 shows the phase component of the impedance of an antenna coupled to a 25-turn hybrid coil (a 1mm-diameter and 2.5mm-length ferrite core solenoid) attached to a humidity sensor. We see that we get a phase dip of 4 degrees and a frequency spread at half dip of 0.4 MHz. The resonance frequency of the LC tank was measured directly and it was confirmed that this frequency corresponds exactly to the frequency at which the phase dip is maximum.

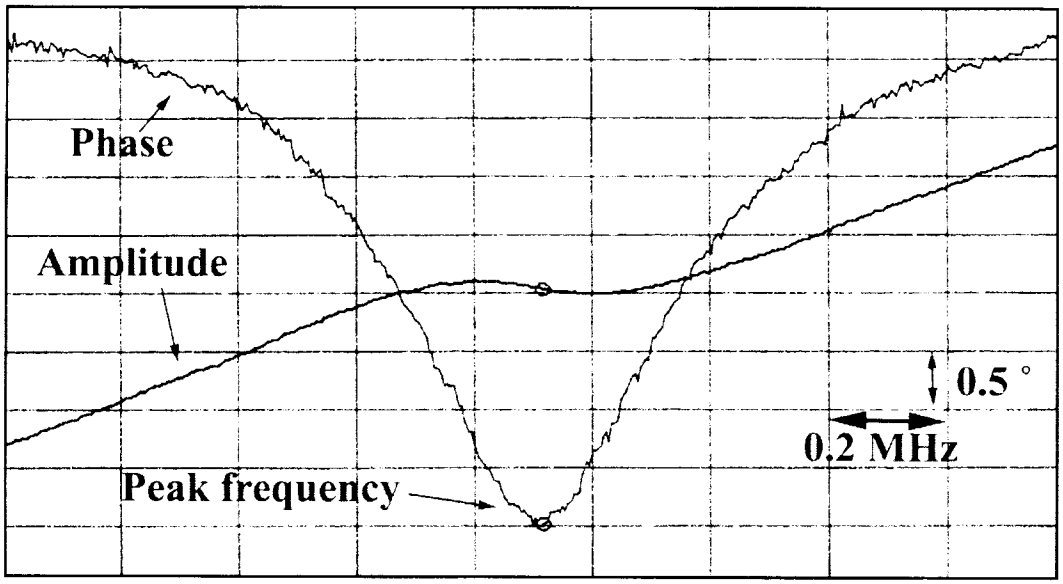

Figure 17: Phase/Amplitude response of the external antenna coupled to a 25-turn hybrid solenoid coil in parallel with a 1200 Å polyimide humidity sensor.

Response to changes in humidity

The response of the system to humidity changes is shown in Figure 18. It shows the phase component obtained when measuring the impedance of a simple one-turn antenna coupled to a humidity sensor-hybrid coil system. Both measurements are made at room temperature, at a relative humidity (RH) of 20%RH (the peak is at a frequency of approximately 5.1 MHz) and 80%RH (peak at approximately 4.5 MHz). Since the phase of the antenna alone is slightly increasing at these frequencies (the simulations did not include any resistance or capacitance for the antenna), a better reading is obtained by plotting the amplitude of the phase dip, as given by Equation 7:

Amplitude of the phase dip	=	Phase of the antenna alone	–	Phase of the antenna coupled to the hybrid coil / humidity sensor	(Eq. 7)

The obtained result is illustrated in Figure 19 (which corresponds to Eq. 7 applied to the curves shown on Figure 18).

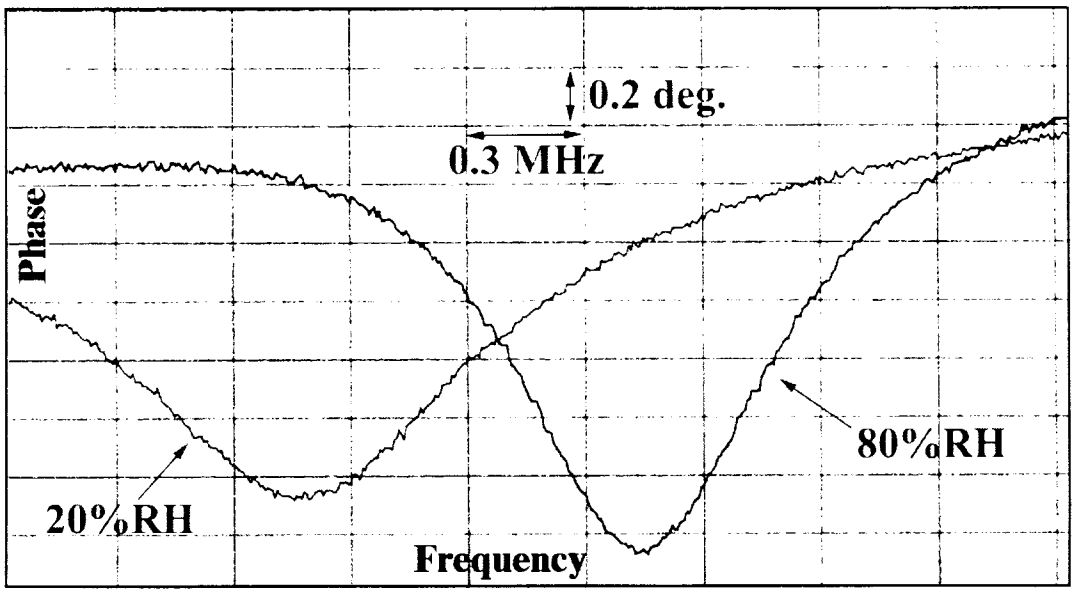

Figure 18: Phase response of the antenna at 20%RH and 80%RH humidity.

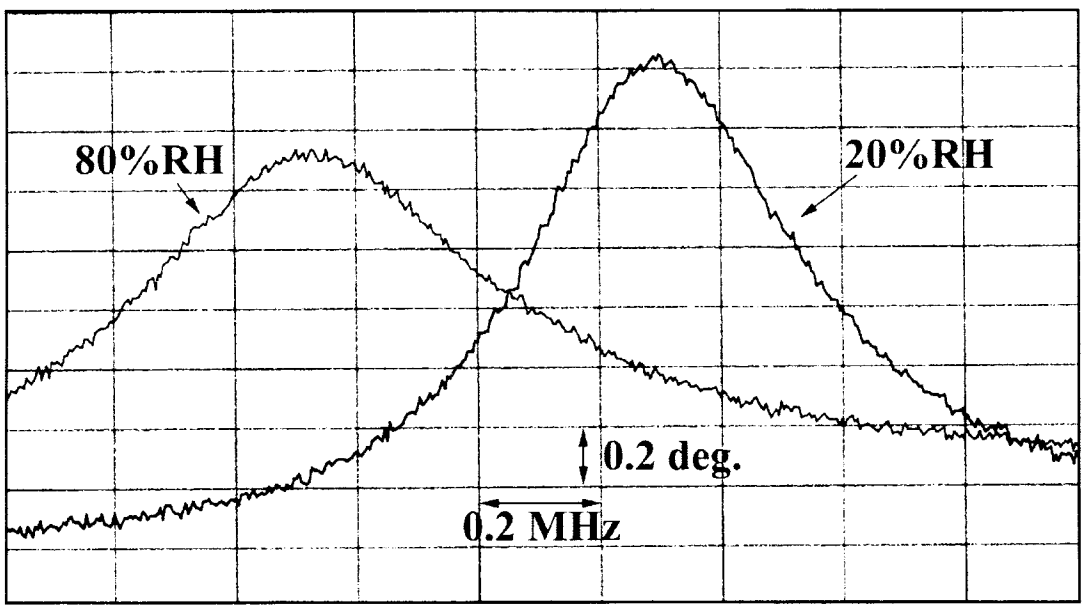

Figure 19: Amplitude of the dip corresponding to Figure 18.

The temperature of the environmental chamber was set to 37°C (human body temperature) and the phase of the antenna (coupled to the hybrid coil-humidity sensor inside the chamber) was measured from 20% to 80% RH with 10% intervals.

The frequency of the peak was recorded both using the phase plot alone, and using the phase dip amplitude (Eq. 7). Table 4 shows the obtained results. Figure 20 shows the plot of the humidity versus the peak frequency obtained from the phase dip amplitude plot.

Table 4: Results from the humidity chamber tests.

Relative Humidity (%RH)	Peak frequency recorded from the phase plot	Peak frequency recorded from the dip amplitude plot (cf. Eq. 1)
20%	4.99 MHz	5.0325 MHz
30%	4.91 MHz	4.9475 MHz
40%	4.84 MHz	4.865 MHz
50%	4.77 MHz	4.820 MHz
60%	4.70 MHz	4.7100 MHz
70%	4.62 MHz	4.645 MHz
80%	4.54 MHz	4.5525 MHz

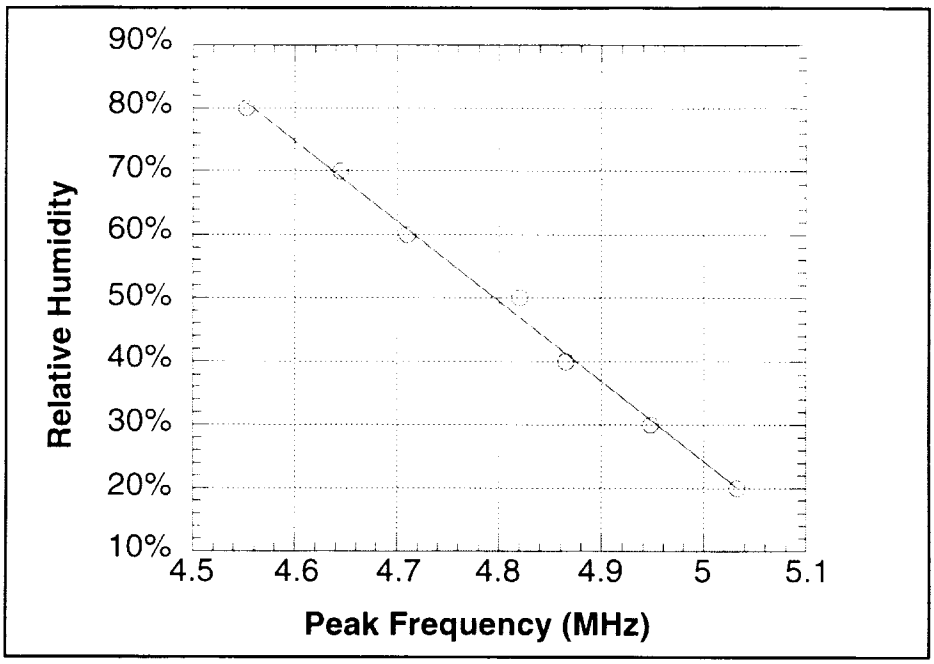

Figure 20: Relative Humidity versus peak frequency (using the dip amplitude plot).

Sensitivity

One application for the wireless humidity sensing system is to monitor the hermeticity of the packages while the Si-Glass package is implanted inside an animal host. It is thus important that the coupling between the antenna and the internal coil is still high enough, when the 2 coils are separated approximately 1cm apart. This is important in order to have an accurate reading of the frequency of the maximum amplitude of the phase dip, which corresponds to the resonance frequency of the humidity sensor system. Also, the measurement should be insensitive to liquid solutions, like saline or body fluids between the 2 coils. Figure 21 shows an amplitude dip plot obtained from a rectangular coil-humidity sensor inside a bonded package, soaked in water, measured with an antenna placed at a distance of 1.2cm away from the package. We can observe a phase dip of 100-200 milli-degrees. The resonance frequency can hence be determined with a

resolution of at least ±20kHz (The actual resolution is better than this). The frequency shift due to humidity is then obtained. From the humidity chamber tests, we achieved sensitivities of 50-80kHz per 10% change of relative humidity, which gives a resolution of the measured relative humidity change better than ±5% RH.

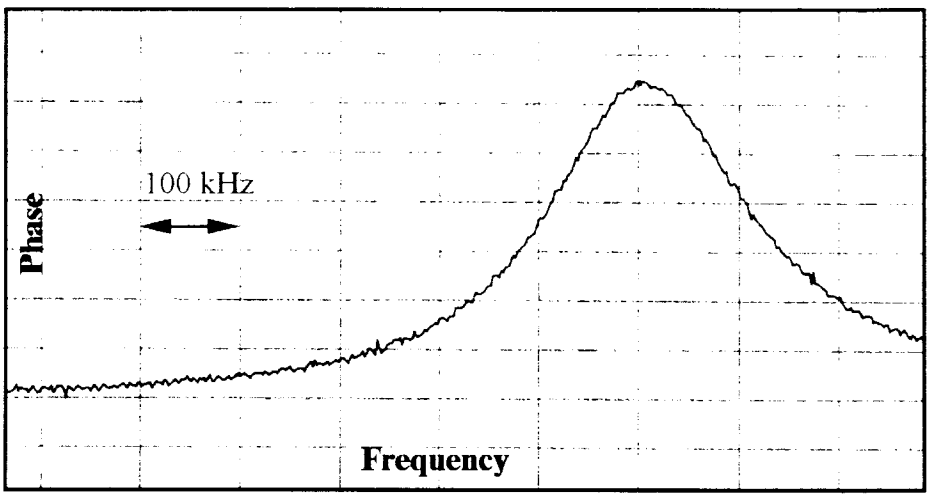

Figure 21: Dip amplitude for a package-antenna distance of 1.2cm.

2.4.4 Summary

We developed a wireless humidity monitoring system which can detect a humidity change of 5% RH inside a package placed up to 2cm away from an external antenna. The resolution is high enough to detect package leakage either in in-vitro or in-vivo (implant) testing. This system was placed inside a package which was anodically bonded. The humidity sensing system is found to operate satisfactorily after bonding.

Since the system operation has been validated in-vitro, we will fabricate new packages equipped with the wireless humidity sensor and use these packages in implants to monitor in-vivo the hermeticity of our micropackages in the coming quarter. We will also use some packages for our in-vitro tests.

2.5 Design and Testing of External Transmitter

In the past quarter, we also started to build a more robust and higher frequency (i.e., 4MHz) class-E transmitter for use with fully-integrated telemetry systems. The schematic of the transmitter is shown in Figure 22. As can be seen, there are three basic parts: the class-E amplifier, the modulation circuitry and the feedback circuitry. The class-E amplifier is similar to the design discussed in previous reports. A feedback network is added to make the class-E based amplifier self-oscillating. The drive coil inductance changes as a result of warping of the coil geometry, loading due to proximity of objects outside the coil, changes in temperature, etc., thus using feedback to maintain the proper drive frequency as the coil inductance changes is crucial. C_{div} is used as a capacitive voltage divider and can sense the coil current. The signal from C_{div} is then sent through a 45° phase delay block and, finally, to a zero crossing detector to provide a feedback signal to the NMOS switch. The component values are:

f= 4MHz; L_{choke}=64μH; L_t=25μH; R_p=1.3Ω; C_t=47pF; C_{div}=5nF; R_{delay}=40Ω; C_{delay}=1nF.

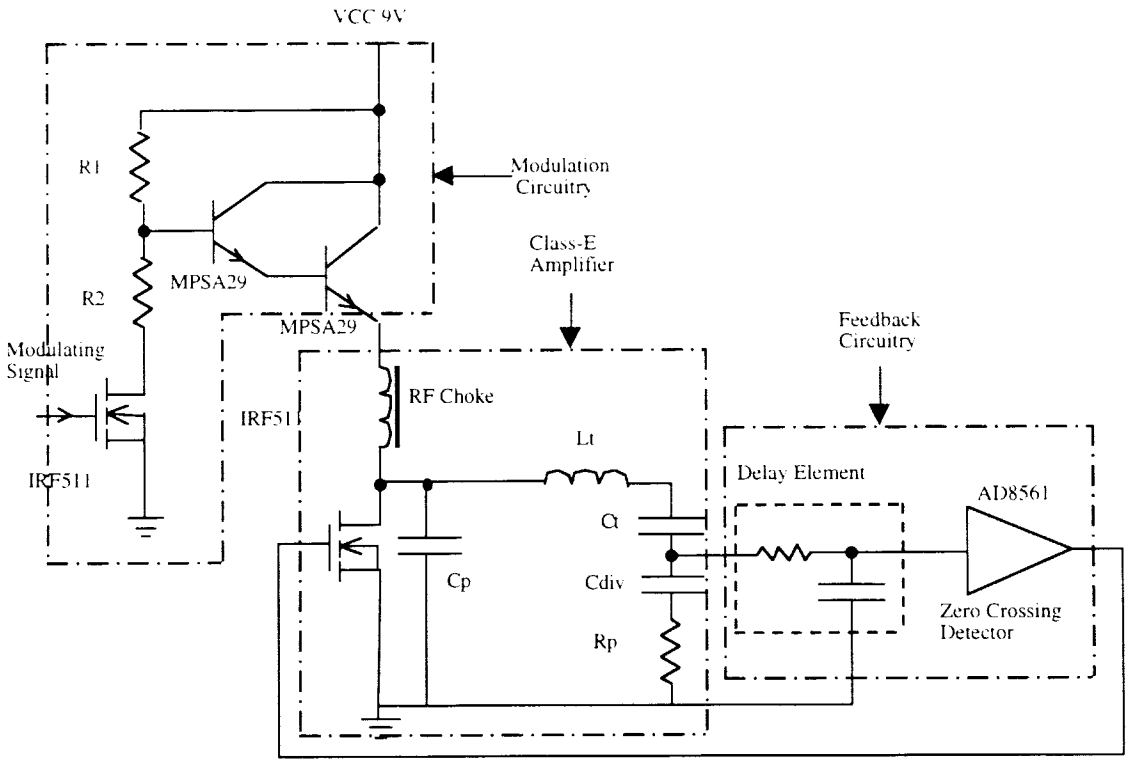

Figure 22: Circuit diagram of the external transmitter.

The transmitter for the microstimulator was designed to work around 2MHz. However, the most recently designed fully integrated system requires a transmitter to operate at 4MHz and hence the old transmitter was modified to operate at this frequency. At this high frequency, parasitic capacitances and inductances from the components and the breadboard can easily disrupt circuit operation, so it is crucial to carefully choose each component in the circuit. In this present design, IRF511 is chosen as the switch. It has small input and output capacitance (C_{ISS}=135pF, C_{OSS}=80pF) and nanosecond switching speed (the rise time and fall time is 10~30ns). In addition, it has high drain to source breakdown voltage (100V). AD8561 is chosen as the comparator used in the zero crossing detector since it has very small delay time (~10ns) and can work with a single supply. Figure 23 shows the waveforms of the drain and gate of the switch. The ripples in the waveforms are caused by the parasitic capacitances coming from the switch itself and the breadboard.

In this design, we use amplitude modulation instead of frequency modulation since the frequency modulation method has lower efficiency compared with amplitude modulation. Amplitude modulation can be accomplished by modulating the supply voltage. The modulating signal drives the switching transistor ON and OFF, therefore changes the supply voltage of the class-E amplifier. The resistors R1 and R2 can be chosen to satisfy different modulation requirements. For example, by choosing R1=200Ω, R2=1kΩ, 20% AM modulation can be achieved with 9V supply voltage. Figure 24 is the Amplitude Modulated signal (10kHz) picked up by a receiver in the middle of the coil. Higher efficiency and lower noise in the external transmitter are desired for improved reliability. In the coming quarter, the efficiency of the transmitter will be tested. A PCB for this circuit will also be fabricated and the transmitter will be tested further.

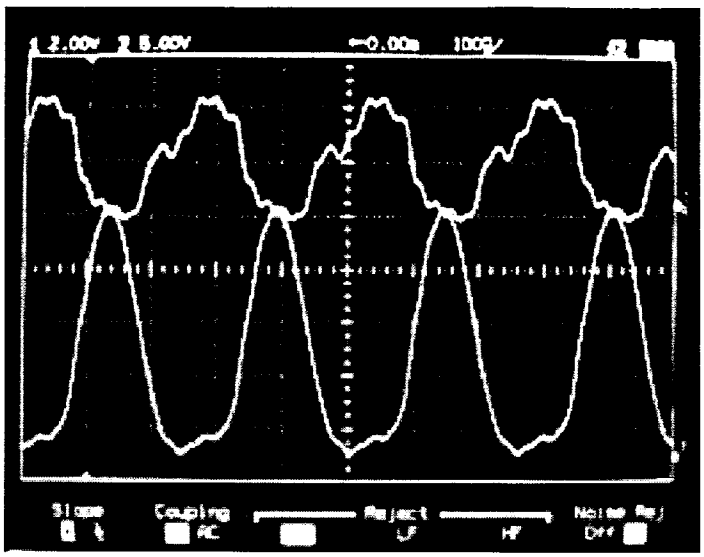

Figure 23: Gate (upper plot) and drain voltage (lower plot) for the NMOS switch.

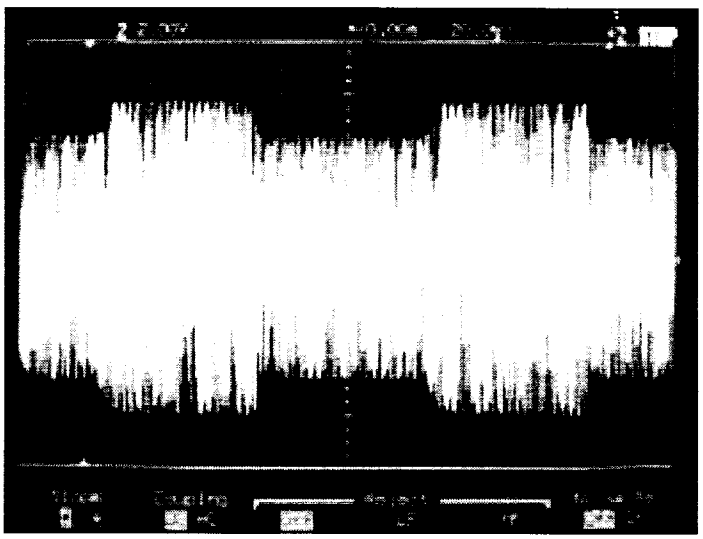

Figure 24: Amplitude modulated signal (10KHz) picked up by a receiver.

III. PLANS FOR THE COMING QUARTER

In the coming quarter, we will use wireless hybrid coil-humidity sensor system by incorporating it into several glass-silicon packages and implanting these into animal hosts. We will continue our efforts to prevent the dissolution of the polysilicon layer using Boron doping via ion implantation. We will also continue fabricating more substrates and prepare more glass-silicon packages for further mechanical tests. A printed circuit board for the transmitter will be designed and fabricated in house. With this, we hope to improve the performance of the transmitter and deliver transmitters to interested users of fully integrated stimulation systems. We will also pursue several paths to generate a low profile Silicon-to-Silicon bond using different metal systems at a relatively low temperature.

References

[1] A. Bohg, "Ethylene Diamine-Pyrocatechol-Water Mixture Shows Etching Anomaly in Boron-Doped Silicon," J. Electrochem. Soc., 118, pp. 401-402, Jan. 1971.

[2] Y. Gianchandani and K. Najafi, "A Bulk Silicon Dissolved Wafer Process for Microelectromechanical Devices," J-MEMS'99, vol.1, no.2, pp. 77-85, June 1992.

[3] K. Najafi, K. D. Wise, and T. Mochizuki "A High-Yield IC-Compatible Multichannel Recording Array," IEEE Trans. Electron Dev., vol.ED-32, no.7 pp. 1206-11, July 1986.

[4] C. Huang and K. Najafi, "Ultra-thin p^{++} Monocrystalline Silicon Microstructures," Solid-State Sensor and Actuator Workshop '98, pp. 241-4, June 1998.

[5] M. Dokmeci and K. Najafi, "A High-Sensitivity polyimide Humidity Sensor for Monitoring Hermetic Micropackages," MEMS'99, pp. 279-284, Jan. 1999.

[6] S. Hauvespre, M. Dokmeci and K. Najafi, "Wireless Humidity Monitoring in Hermetic Biomedical Micropackages", submitteed to The EMBS/BMES 99 Conference.

[7] F. T. Ulaby, *Fundamental of Applied Electromagnetics*, Prentice Hall, New Jersey, 1997.